Alkyl Selenide− and Alkyl Thiolate−Functionalized Gold Nanoparticles: Chain Packing and Bond Nature

ARTICLE *in* LANGMUIR · SEPTEMBER 2003

Impact Factor: 4.46 · DOI: 10.1021/la020628i

6 AUTHORS, INCLUDING:

Abraham Ulman
Polytechnic Institute of New York University
92 PUBLICATIONS **11,848** CITATIONS
SEE PROFILE

Atul N Parikh
University of California, Davis
175 PUBLICATIONS **6,882** CITATIONS
SEE PROFILE

Miriam Rafailovich
Stony Brook University
226 PUBLICATIONS **3,056** CITATIONS
SEE PROFILE

Alkyl Selenide- and Alkyl Thiolate-Functionalized Gold Nanoparticles: Chain Packing and Bond Nature

Chanel K. Yee,[†,⊥,||] Abraham Ulman,*[,†,⊥] Julia D. Ruiz,[‡] Atul Parikh,[‡,||] Henry White,[§,⊥] and Miriam Rafailovich[§,⊥]

Department of Chemical Engineering and Chemistry, Polytechnic University, Six Metrotech Center, Brooklyn, New York 11201, JDR & ANP, Bioscience Division, Los Alamos National Laboratory, Los Alamos, New Mexico 87545, Department of Materials Sciences and Engineering, State University of New York at Stony Brook, Stony Brook, New York 11794-2275, and NSF MRSEC for Polymers at Engineered Interfaces

Received July 11, 2002. In Final Form: June 16, 2003

We have studied the effects of relative mole ratios of the reactant precursors in the one-phase synthesis of alkaneselenoate- and alkanethiolate-functionalized gold nanoparticles. Specifically, we prepared a series of dodecaneselenoate (DDSe)- and dodecanethiolate (DDT)-functionalized gold nanoparticles using four different Se/Au and S/Au mole ratios in reactant mixtures at two different reaction temperatures employing three different solvents. In all cases, the synthesis relied on the reduction of $H[AuCl_4]$, in the presence of dodecanethiol (DDT) and didodecyl diselenide (DD_2Se_2) using lithium triethylborohydride (superhydride) as the reducing agent. Nanoparticle formation, structure, and bonding characteristics were investigated using a combination of transmission electron microscopy, UV absorption spectroscopy, thermogravimetric analysis, Fourier transform infrared spectroscopy, and X-ray photoelectron spectroscopy. Passivation by alkyl selenide was more efficient and was characterized by greater chain density and stronger Au−Se bond strength when high ligand/substrate ratios were employed. Particle size was surprisingly uniform in all cases, independent of mole ratio. By contrast, particle size (2−5 nm) was found to increase with increasing mole ratios when the passivating ligand was alkanethiolate, whose chain grafting density increased with increasing mole ratio, fully coincided with the literature. These results can be reconciled in terms of a simple mechanistic scenario wherein the nanoparticle formation using alkanethiolate ligands proceeds via the formation of a "polymer-like" intermediate between the Au ions and the alkanethiolate ligands prior to reduction whereas such an intermediate is not formed when selenoate is used as the binding ligand.

Introduction

Within the growing and increasingly more complex area of nanotechnology,[1] nanoparticles have become a significant focal point of activity. This is because the confinement and quantum effects that dominate nanoparticle behavior render their material properties significantly different from those of their bulk counterparts. Furthermore, a wide variety of nanoparticles can be controllably synthesized. As a result, they provide interesting materials for the fundamental explorations of size-dependent and nanoscale phenomena. Their technological importance stems from their novel and useful structural, optical, and functional properties.[2] In this regard, gold nanoparticles have emerged as prototypical models of metal nanoparticles with wide-ranging applications. They have been used as substrates for well-defined, high-density polymer brushes by surface-initiated living radical polymerization,[3] as centers in networks,[4] as catalysts' oxide supports,[5] and as sensors.[6] Gold nanoparticles are also finding new broad applications in bioscience including their use as substrates for DNA attachment,[7] as signal amplifiers for biological recognition, and as mediators in transfection of mammalian cells.[8]

In the synthesis of gold nanoparticles, to date, organosulfur derivatives have provided the most widely used ligands. Specifically, most previous studies have focused on alkanethiolate-functionalized gold nanoparticles, but the use of dialkyl sulfides has also been reported,[9] presumably because of their widespread use as self-assembling molecules at gold surfaces. In this vein, organoselenoates provide a useful alternative. The formation of stable, well-defined self-assembled monolayers

* Corresponding author. Phone: (718) 260-3119 (O), (718) 260-3125 (F). E-Fax: (810) 277-6217. E-mail: aulman@duke.poly.edu.

|| Present address: Department of Applied Science, University of California Davis, 1 Shields Avenue, Davis, CA 95616-8254.

† Polytechnic University.

‡ Los Alamos National Laboratory.

§ State University of New York at Stony Brook.

⊥ NSF MRSEC for Polymers at Engineered Interfaces.

(1) Murphy, C. J.; Arkin, M. R.; Jenkins, Y. I.; Ghatlia, N. D.; Bossmann, S. H.; Turro, N. J.; Barton, J. K. *Science* **1997**, *262*, 1025. (b) Wang, J.; Palecek, E.; Nielsen, P. E.; Rivas, G.; Cai, X.; Shiraishi, H.; Donta, N.; Luo, D.; Farias, P. *J. Am. Chem. Soc.* **1996**, *118*, 7667. (c) Wang, J.; Fermandes, J. R.; Kubota, L. T. *Anal. Chem.* **1998**, *70*, 3699. (d) Uddin, A. H.; Plunno, P. A.; Hudson, R. H.; Damha, M. J.; Krull, U. *J. Nucleic Acids Res.* **1997**, *25*, 4139. (e) Fang, X.; Liu, X.; Schuster, S.; Tan, W. *J. Am. Chem. Soc.* **1999**, *121*, 2921. (f) Millan, K. M.; Mikkelsen, S. R. *Anal. Chem.* **1993**, *65*, 2317.

(2) Wang, J.; Rivas, G.; Cai, X.; Shiraishi, H.; Donta, N.; Luo, D.; Farias, P. *Anal. Chem.* **1996**, *68*, 2629. (b) Bohrmann, B.; Kellenberger, E. J. *Histochem. Cytochem.* **1994**, *42*, 635. (c) Hall, D. B.; Holinlin, R. E.; Barton, J. K. *Nature* **1996**, *382*, 731.

(3) Jordan, R.; West, N.; Ulman, A.; Chou, Y.-M.; Nuyken, O. *Macromolecules* **2001**, *34*, 1606. (b) Ohno, K.; Koh, K.-m.; Tsujii, Y.; Fukuda, T. *Macromolecules* **2002**, *35*, 8989.

(4) Wang, T.; Zhang, D.; Xu, W.; Li, S.; Zhu, D. *Langmuir* **2002**, *18*, 8655.

(5) Haruta, M. *Catal. Today* **1997**, *36*, 153.

(6) Jia, J.; Wang, B.; Wu, A.; Cheng, G.; Li, Z.; Dong, S. *Anal. Chem.* **2002**, *74*, 2217. (b) Liu, T.; Tang, J.; Zhao, H.; Deng, Y.; Jiang, L. *Langmuir* **2002**, *18*, 5624. (c) Lindblad, M.; Lestelius, M.; Johansson, A.; Tengvall, P.; Thomsen, P. *Biomaterials* **1997**, *18*, 1059. (d) Niemeyer, C. M.; Boldt, L.; Ceyhan, B.; Blohm, D. *Anal. Biochem.* **1999**, *268*, 54.

(7) Storhoff, J. J.; Elghanian, R.; Mirkin, C. A.; Letsinger, R. L. *Langmuir* **2002**, *18*, 6666.

(8) Sandhu, K. K.; McIntosh, C. M.; Simard, J. M.; Smith, S. W.; Rotello, V. M. *Bioconjugate Chem.* **2002**, *13*, 3.

(9) Shelley, E. J.; Ryan, D.; Johnson, S. R.; Couillard, M.; Fitzmaurice, D.; Nellist, P. D.; Chen, Y.; Palmer, R. E.; Preece, J. A. *Langmuir* **2002**, *18*, 1791.

10.1021/la020628i CCC: $25.00
Published on Web 09/25/2003

(SAMs) of alkaneselenoates on polycrystalline gold films was first reported by Samant and co-workers[10a] and has since been characterized by many at polycrystalline and single crystal gold surfaces. Alkaneselenols and dialkyl diselenides are now known to organize at the gold surface to form stable single monolayers in an incommensurate packing wherein the aliphatic chains organize in an ordered conformation at high densities presenting a cant angle of approximately 15° from the surface normal. To the best of our knowledge, however, their use in the synthesis of gold nanoparticles has not been explored.

The use of alkaneselenols and particularly dialkyl diselenides in the nanoparticle synthesis is potentially attractive for two reasons. First is the bonding preference. Since the Se−Se is a weaker bond than S−S (42 vs 54 kcal mol^{-1}, respectively), it can be expected that oxidative addition of the Se−Se bond to gold should be more favorable and facile. Moreover, selenium is slightly less electronegative than sulfur (2.55 vs 2.58 Pauling units) and larger in size (1.98 vs 1.84 Å); One would, therefore, expect a stronger selenoate (soft base)−gold(I) (soft acid) bonding. Second are the chain-structural properties. The aliphatic chains of alkaneselenoates have been previously shown to yield a packing assembly considerably denser than that of alkanethiol monolayers on gold.[10] While the latter (alkanethiolates) adopt a close packed chain configuration at 30° tilt, alkaneselenoates pack in a distorted hexagonal configuration at a considerably lower tilt of about 15°. It appears that this stronger substrate−headgroup binding and denser chain packing for alkaneselenoates can be exploited to gain some synthetic control of the structure and properties of gold nanoparticles.

In this paper, we present the one-phase preparation[11] and characterization of alkaneselenoate passivated gold nanoparticles. We also provide a detailed study of the effects of the ligand to substrate precursor ratios on nanoparticle structure and properties and carry out a direct comparison of their morphological, structural, and bonding preferences with their alkanethiolate counterparts.

Experimental Section

Chemicals. All chemicals were purchased from Aldrich and used as received except didodecyl diselenide, which was synthesized in our laboratory. Solvents were obtained from EM Science or Aldrich. Tetrahydrofuran (THF) used for the synthesis was freshly distilled to remove the stabilizer and further dried by molecular sieves.

Preparation of DDSe/Au and DDT/Au Nanoparticles. Four Se/Au (and S/Au) mole ratios have been synthesized: 2:1, 1:1, 1:2, and 1:3. Four samples of 99.2 mg (0.2 mmol) didodecyl diselenide ($C_{12}H_{25}Se-SeC_{12}H_{25}$, DD_2Se_2) were each added to vigorously stirred solutions of 0.2, 0.4, 0.8, and 1.2 mmol of hydrogen tetrachloroaureate(III) trihydrate ($HAuCl_4 \cdot 3H_2O$), in 20 mL of freshly distilled anhydrous THF, at 6 °C, under N_2 purge. In a similar fashion, four samples of 80.8 mg (0.4 mmol) of dodecanethiol ($C_{12}H_{25}SH$, DDT) in 20 mL of freshly distilled anhydrous THF were each mixed with solutions of 0.2, 0.4, 0.8, and 1.2 mmol of $HAuCl_4 \cdot 3H_2O$, respectively, under vigorous stirring. Each reaction mixture was stirred for 2 h, before 1.0 M of lithium triethylborohyride (superhydride) in THF was added dropwise. The addition rate was adjusted to maintain the reaction temperature of 6 ± 1 °C. Gas evolution and color changes were immediately observed in each of the reaction flasks upon addition of the reducing agent. The addition of superhydride (in excess[12]) was terminated when no more H_2 gas evolved and the reaction temperature did not increase. The reaction mixtures were stirred for an additional 2 h to ensure reaction completion. Each resulting solution mixture was centrifuge with ethanol to remove excess thiol or diselenide, as confirmed by thin-layer chromatography (TLC, with hexane as the eluent). After centrifugation, the supernatant was discarded. The purified nanoparticles were dried in a vacuum desiccator overnight. Pure nanoparticles can be resuspended in chloroform.

Elemental Analysis. Samples of four mole ratios of Au/DDSe nanoparticles were sent to Galbraith Laboratories, Inc. (Knoxville, TN) for inductively coupled plasma optical emission spectroscopy (ICP-OES). Percentages of carbon, hydrogen, gold, and selenium in 2:1, 1:1, 1:2, and 1:3 mole ratios were obtained respectively as the following: 29.19%, 5.11%, 49.23%, 16.36%; 23.35%, 3.82%, 60.16%, 13.12%; 3.78%, 0.65%, 93.39%, 2.00%; 1.92%, <0.5%, 95.78%, 0.98%.

Transmission Electron Microscopy (TEM). Thin films of each sample in chloroform were drop cast onto 300-mesh carbon-supported film copper grids. A Phillips CM-12 transmission electron microscope (100 keV) was used to determine the average particle size for each sample measured. An NIH imager (Beta 3 release) was used to determine the interparticle spacing. A particle size distribution histogram was established after computer pixel counting of over 100 nanoparticles in each sample, followed by the mathematical conversion based on a standard pixel−micrometer scale.

X-ray Photoelectron Spectroscopy (XPS). XPS results were obtained using a Kratos ES300 X-ray photoelectron spectrometer with a nonmonochromatic Mg Kα X-ray source (1253.6 eV photons). The hemispherical energy analyzer was operated in the fixed retardation ratio mode. The samples were drop cast on Silicon substrates, which were in turn mounted on standard sample studs by means of double-sided adhesive tape and subsequently dried in a vacuum oven. The pressure in the analysis chamber was $\sim 10^{-8}$ Torr during measurements. Core level C 1s, Se 3d, S 2p, and Au 4f spectra were monitored at an electron takeoff angle of 15°. To compensate for surface charging effects, all binding energies were referenced to the C 1s neutral carbon peak at 285.0 eV. Deconvolution of complex peaks in each element was performed using an Origin nonlinear curve fit in which underlying peaks were separated and integrated while accounting for the correction of peak intensities based on the Scofield correction factors in conjunction with the standard line position table as the reference.

Infrared Spectra. Infrared spectra were collected using a Bruker IFS55 Fourier transform infrared spectrophotometer equipped with a DTGS detector (Bruker, Göttingen, Germany). The sample consisted of pellets prepared by pressing a mechanically homogenized mixture of nanoparticles with nominally dehydrated pure KBr. The spectra were obtained in a 2 cm^{-1} resolution. For more precise determination of peak positions, the interferrograms were zero-filled to increase the point density by a factor of 2. All spectra are reported in transmission absorbance units, $[A = -\log(T/T_o)]$, where T and T_o are the power spectra of each sample and reference, respectively. The data analysis was performed using Grams 32 (SpectraCalc) and Origin software packages for curve fitting and analyses.

Thermal Gravimetric Analysis. The samples (~10 mg) were heated to 800 °C at a rate of 10 °C/min under a nitrogen atmosphere. A thermal gravimetric analyzer model 2920 from TA Instruments was used.

UV−Visible Absorption Spectroscopy. All experiments were performed in the temperature-controlled chamber (25 ± 0.1 °C) of a UV−visible spectrophotometer (model 1601) from Shimadzu Scientific Instrument. A small amount of solution was removed via syringe and diluted to a required optical density with the addition of THF.

(10) Samant, M. G.; Brown, C. A.; Gordon, J. G., II. *Langmuir* **1992**, *8*, 1615. (b) Bandyopadhyay, K.; Vijayamohanan, K. *Langmuir* **1999**, *15*, 5314. (c) Bandyopadhyay, K.; Vijayamohanan, K. *Langmuir* **1998**, *14*, 625. (d) Koji, N.; Takeshi, S.; Masato, T.; Makoto, T. *Langmuir* **2000**, *16*, 2225. (e) Huang, F. K.; Horton, R. C.; Myles, D. C.; Garrell, R. L. *Langmuir* **1998**, *14*, 4802.

(11) Yee, C. K.; Jordan, R.; Ulman, A.; White, H.; King, A.; Rafailovich, M.; Sokolov, J. *Langmuir* **1999**, *15*, 3486. (b) Yee, C.; Scotti, M.; Ulman, A.; White, H.; Rafailovich, M.; Sokolov, J. *Langmuir* **1999**, *15*, 4314.

(12) According to Brust and co-workers,[4] the reducing hydride should be 12 times as much as the amount of $HAuCl_4$ to ensure complete reduction.

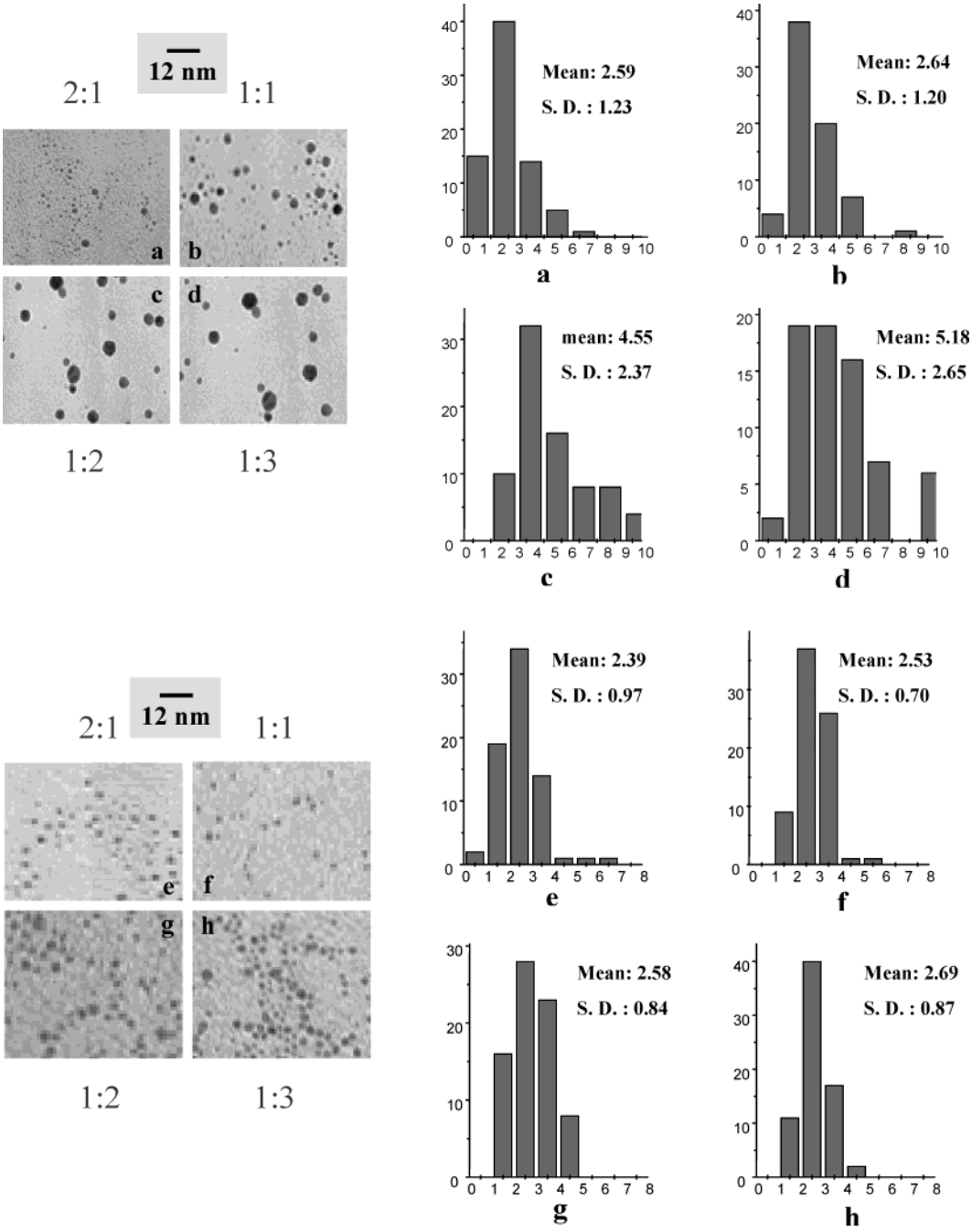

Figure 1. TEM images and histograms of Au/DDT (a−d) and Au/DDSe (e−h) nanoparticles prepared using four ligand-to-gold molar ratios.

Results

For both alkanethiolate and alkaneselenoate ligands, Au nanoparticles form at all mole ratios, at both reaction temperatures (6 and 25 °C) and using all solvents employed in the present study. Alkaneselenoates and alkanethiolates yield comparable nanoparticles that exhibit dark brown or purple color depending on the reaction conditions used. Below, we describe results of our spectroscopic and microscopic investigations of the detailed structures of DDT/Au and DDSe/Au nanoparticles.

Typical TEM images for DDSe/Au and DDT/Au nanoparticles prepared using four different ligand to substrate mole ratios are shown in Figure 1. Even a casual inspection of the data reveals that in the case of DDT/Au, as the S/Au mole ratio decreased from 2:1 to 1:1 to 1:2 to 1:3, the average particle sizes increased, while no such noticeable trend was observed for DDSe/Au.

A careful examination of DDT/Au results using size histograms, also shown in Figure 1a−d, derived by analyzing several TEM micrographs reveals the average particle size was the smallest (2.59 nm) and the distribution the narrowest (sd 1.23) for the S/Au ratio 2:1 in the reactant mixture. As the S/Au mole ratio decreased, the average particle size increased from 2.59 nm for a 2:1 mole ratio to 5.18 nm for a 1:3 mole ratio with a concomitant broadening in the size distribution as measured by an increased particle size standard deviation from 1.23 to 2.65. These observations are in good general agreement with previous studies,[13] where it was observed that the gold nanoparticles tended to get larger as the S/Au mole ratio decreased. By contrast, for the DDSe/Au

(13) Hostetler, M. J.; Murray, R. W. *Curr. Opin. Colloid Interface Sci.* **1997**, *2*, 42. (b) Hostetler, M. J.; Wingate, J. E.; Murray, R. W. *Langmuir* **1998**, *14*, 17.

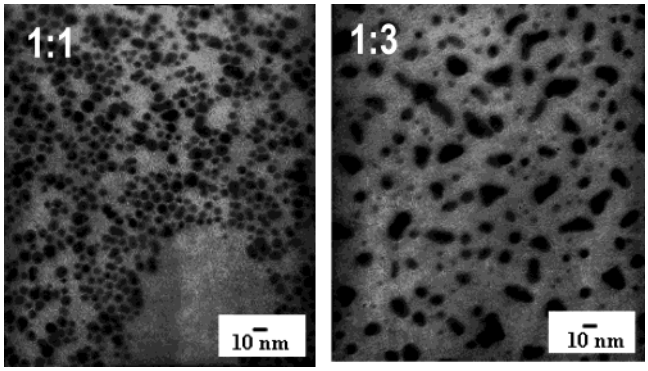

Figure 2. TEM images of Au/DDSe nanoparticles made in toluene/water in 1:1 and 1:3 mole ratios.

analogues (Figure 1e−h), the particle size characteristics displayed a dramatically different behavior as Au/Se ratios were changed. Specifically, the average sizes (2.39−2.69 nm) of the resultant particle were not affected to any significant extent by the changes in the ligand/substrate mole ratio, and the size distribution was uniform (sd 0.97−0.87) for all mole ratios. *Thus, by simply varying the reactant mole ratios in the one-phase synthesis, a control and tunability in particle dimensions for DDS/Au can be achieved whereas such tunability is not afforded in the DDSe/Au case.*

Next, we monitored the particle size and size distribution of DDSe/Au nanoparticles following a two-phase (toluene/H_2O) synthesis procedure. TEM data in Figure 2 illustrate the particles produced using DDSe and Au in [1:1] and [1:3] mole ratios in reactant mixtures. For the 1:1 mole ratio case, the nanoparticles are ∼7 nm in diameter, whereas, for the 1:3 case, the nanoparticles exhibited a wide range of irregular shapes and sizes. These observations sharply differ from the small, uniform, and mole ratio independent sizes of DDSe/Au nanoparticles observed in the one-phase THF synthesis (Figure 1f and h). We note that thiolate-functionalized nanoparticles such as produced here or by other methods reported in the literature have not yielded such significant variations in sizes and size distributions dependent on mole ratios. Most of the alkanethiolate-functionalized gold nanoparticles reported in the literature maintained their isotropic "spherical" shape even when the RSH/Au ratio was as low as 1:12.[13b,14]

Ultraviolet−visible (UV−vis) absorption spectra of DDSe/Au and DDT/Au are shown in Figure 3. The traces reveal two major bands. The longer wavelength peak with maxima at ∼500 nm can be straightforwardly attributed to the surface plasmon absorption due to the gold nanoparticles. The second, lower wavelength absorption, at ∼230 nm, has been previously assigned to the Au^+ absorption band. The precise location of the surface plasmon absorption showed a systematic dependence on the reactant mole ratios for both DDSe/Au and DDT/Au nanoparticles. In particular, for DDSe/Au nanoparticles, the peak position showed a gradual blue shift as the DDSe/Au ratio is lowered from 2:1 (531.5 nm) to 1:1 (528.1 nm) to 1:2 (515.7 nm) to 1:3 (512.4 nm). A similar blue shift was also observed for DDT/Au nanoparticles for all reactant mole ratios [1:1 (520 nm), 1:2 (509.1 nm), 1:3 (503.7 nm)] except for the lowest, 2:1, for which the peak could not be detected. Note also that the blue shift in peak maxima above corresponds to the broadening and higher intensities for the plasmon absorption bands as the reactant mole ratios of ligand to Au are lowered.

(14) Fan, C.; Jiang, L. *Langmuir* **1997**, *13*, 3059.

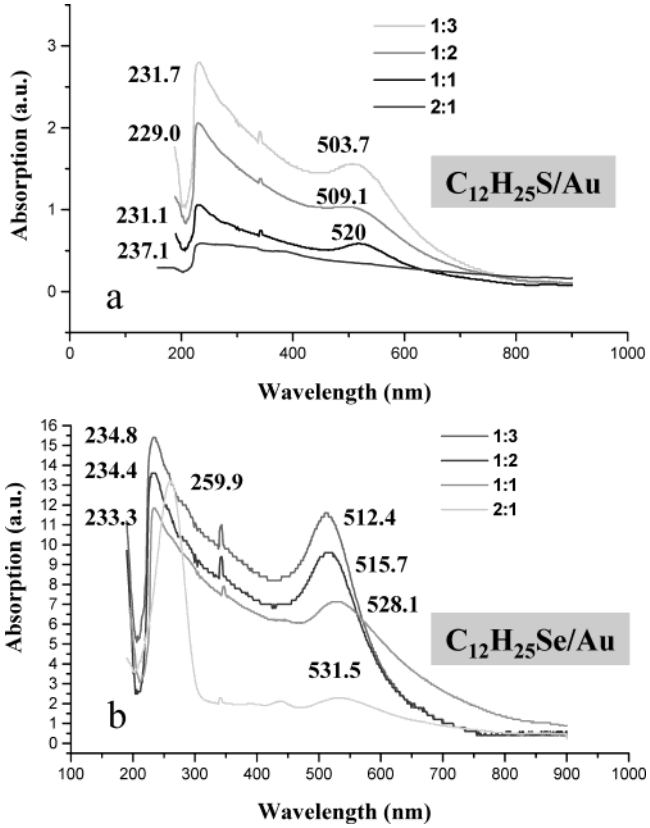

Figure 3. UV spectra of Au/DDSe (a) and Au/DDT (b) nanoparticles prepared using four ligand-to-gold molar ratios.

Previous reports have shown that the relations between surface plasmon peak characteristics (position, width, and intensity) and particle size are generally very complex.[15] The observed shifts in DDT/Au nanoparticles as a function of reactant mole ratios above can be straightforwardly correlated with the decreasing average parti/cle sizes (see TEM data above). For DDSe/Au, however, the observed blue shift in the plasmon bands as mole ratios are changed is intriguing, since the TEM data revealed that the average particle size did not change. We speculate that this behavior is indicative of the variations in ligand−substrate bond.

The thermal stabilities of the DDT/Au and DDSe/Au nanoparticles were characterized using thermogravimetric analysis (TGA). Traces in Figure 4 show TGA weight losses for the DDT/Au (left panel) and DDSe/Au (right panel) series of nanoparticles for the four reactant mole ratios, 2:1, 1:1, 1:2, and 1:3, used in the present study. In all cases, the traces reveal characteristic reverse-sigmoidal curves. For DDT/Au the dominant weight loss occurs at ∼220 °C, which can be attributed to the loss of the organic ligand from the nanoparticle surfaces. This loss can be used as a measure of the organic content (in fractional mass) on particle surfaces. For DDT/Au nanoparticles, these values for the four mole ratios were as follows: 2:1, 46.94%; 1:1, 42.84%; 1:2, 26.36%; 1:3, 20.46%, showing that, with decreasing mole ratio of the reactants, the organic mass loss and hence the ligand coverage on nanoparticles decrease steadily. Similarly, for the DDSe series, the percentage of weight loss or the organic coverage on particle surfaces for 2:1, 1:1, 1:2, and 1:3 ratios was

(15) Link, S.; El-Sayed, M. A. *J. Phys. Chem. B* **1999**, *103*, 4212−4217. (b) Alvarez, M. M.; Khoury, J. T.; Schaaff, G. T.; Shafigullin, M. N.; Vezmar, I.; Whetten, R. L. *J. Phys. Chem. B* **1997**, *101*, 3706−3712. (c) Alvarez, M. M.; Khoury, J. T.; Schaaff, G. T.; Shafigullin, M. N.; Vezmar, I.; Whetten, R. L. *Chem. Phys. Lett.* **1997**, *266*, 91−98.

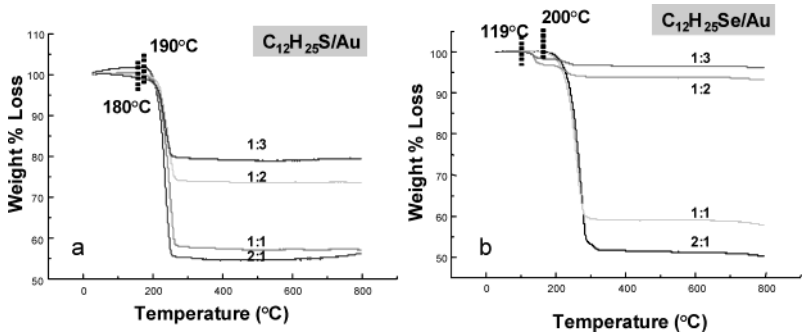

Figure 4. TGA traces of Au/DDT (a) and Au/DDSe (b) nanoparticles prepared using four ligand-to-gold molar ratios.

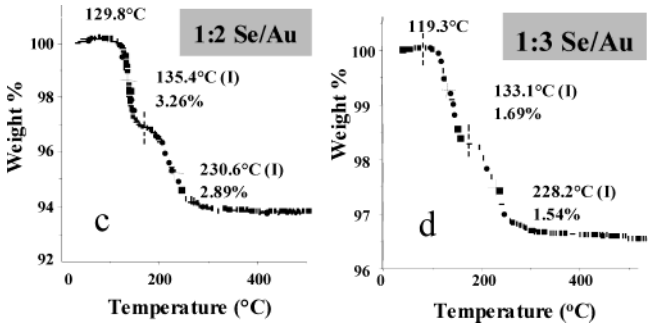

Figure 5. Detailed analysis of Au/DDSe nanoparticles in 1:2 (c) and 1:3 (d) mole ratios.

found to be 48.8%, 40.9%, 6.15%, and 3.23%, indicating decreased ligand coverage with decreasing reactant mole ratios.

Next, we note that the onset desorption temperature for the main transition in TGA was 190 °C for DDT/Au and 200 °C for DDSe/Au, indicating good and comparable thermal stability of both selenoate and thiolate ligands at Au nanoparticles.

A careful examination of the DDSe/Au transition region in the TGA traces (Figure 5) showed a peculiar behavior for low mole ratios. For 1:2 and 1:3 mole ratios, the transition regions revealed a two-step mass loss process involving a first small (10%) mass loss regime at 120−130 °C followed by the main transition at ∼230 °C. For the same mole ratios in the DDSe/Au case, ligand coverages (see above) were also notably lower, indicated by the mass losses of 6.15% and 3.23% coverages for the 1:2 and 1:3 mole ratios (see above). The mechanistic implications of this peculiarity are discussed later in the manuscript.

FTIR spectroscopy was used to ascertain chain conformational and packing characteristics. FTIR spectra for DDT/Au and DDSe/Au nanoparticles prepared using four reactant mole ratios (2:1, 1:1, 1:2, and 1:3) are shown in Figure 6.

We divide our report on FTIR studies into two parts. We start by discussing the results in the 3000−2800 cm^{-1} range. The high-frequency region—between 2800 and 3000 cm^{-1} for all spectra—revealed a characteristic aliphatic chain signature. The signature exhibits three well-resolved peaks in the ∼2850−2854, ∼2917−2922, and 2956−2964 cm^{-1} regions which have been previously assigned to methylene C−H sym, methylene C−H antisym, and methyl asym vibrational absorption bands. Overlapping contributions from weak Fermi resonances and the methyl sym absorption at ∼2878 cm^{-1} create an appearance of overlapping peaks within the signatures.

As a function of the reactant mole ratios, both d+ and d− modes show a shift in peak positions. For the DDT/Au series, as the mole ratios are decreased from 2:1 to 1:1 to 1:2 to 1:3, the positions of the d+ and d− peaks shift gradually from 2848 and 2917 cm^{-1} for the 2:1 case to 2851 and 2920 cm^{-1} for the 1:3 case.

For the DDSe/Au series, the shifts for the same compositions are somewhat less pronounced. For the 2:1 mole ratio case, the peak maxima were estimated at 2919 and 2848 cm^{-1} for the d− and d+ modes, respectively. These positions shifted slightly ($\Delta\upsilon = +1-2$ cm^{-1}) as the mole ratios were lowered. For the lowest mole ratio composition of 1:3 studied here, peak maxima were at 2920 and 2850 cm^{-1}.

It is well appreciated in the past literature[16,17] that the exact locations of the d+ and d− modes are highly sensitive to the spatial conformations of the alkyl chains and statistically proportional to the average trans and gauche methylene populations within the chains. The peak frequencies of the CH_2 stretching modes of alkyl chains are typically reported to lie in the narrow ranges 2846−2850 and 2915−2918 cm^{-1} for all-trans extended chains and in the distinctly different ranges 2854−2856 and 2924−2928 cm^{-1} for conformationly disordered chains characterized by a significant presence of gauche conformers.[18−20] On this basis, the observed peak frequencies for both DDSe/Au and DDT/Au nanoparticles in the relatively narrow ranges 2847−2851 and 2917−2920 cm^{-1} in the spectra of varying mole ratios establish that ligand chains were organized *mostly in the ordered conformational state* with increasing chain disorder evident in the spectra for lower mole/ ratio compositions. For the lowest (1:3) mole ratios, DDT/Au and DDSe/Au exhibited d+ and d− peak positions, respectively, implying that chains are only partially disordered, consistent with a liquid-crystalline-like state rather than fully disordered liquidlike chains.

Turning to the 1500−700 cm^{-1} region, the inferences above regarding chain conformation and its dependence on the mole ratios are further strengthened by the spectral features observed in the lower frequency region. Spectra in the 700−1500 cm^{-1} region, also shown in Figure 6**,** display a rich signature. A series of closely spaced peaks between 1100 and 1300 cm^{-1} due to wag−twist progression modes is a strong indicator of the presence of conformationally ordered chains. These peaks are well-resolved for higher mole ratio compositions (2:1 and 1:1) for both DDT/

(16) Bensebaa, F.; Ellis, T. H.; Badia, A.; Lennox, R. B. *Langmuir* **1998**, *14*, 2361.

(17) Hostetler, M. J.; Stokes, J. J.; Murray, R. W. *Langinuir* **1996**, *12*, 3604. (b) Badia, A.; Cuccla, L.; Demers, L.; Morin, F.; Lennox, R. B. *J. Am. Chem. Soc.* **1997**, *119*, 2682.

(18) Porter, M. D.; Bright, T. B.; Allara, D. L.; Chidsey, E. E. D. *J. Am. Chem. Soc.* **1987**, *109*, 3559.

(19) Macphail, R. A.; Strauss, H. L.; Snyder, R. G.; Elliger, C. A. *J. Phys. Chem.* **1984**, *88*, 334. (b) Snyder, R. G.; Hsu, S. L.; Krimin, S. *Spectrochim. Acta* **1978**, *34*, 395.

(20) Dorset, D. L.; Strauss, H. L.; Snyder, R. G. *J. Phys. Chem.* **1991**, *95*, 938. (b) Snyder, R. G.; Strauss, H. L.; Elliger, C. A. *J. Phys. Chem.* **1982**, *86*, 5145.

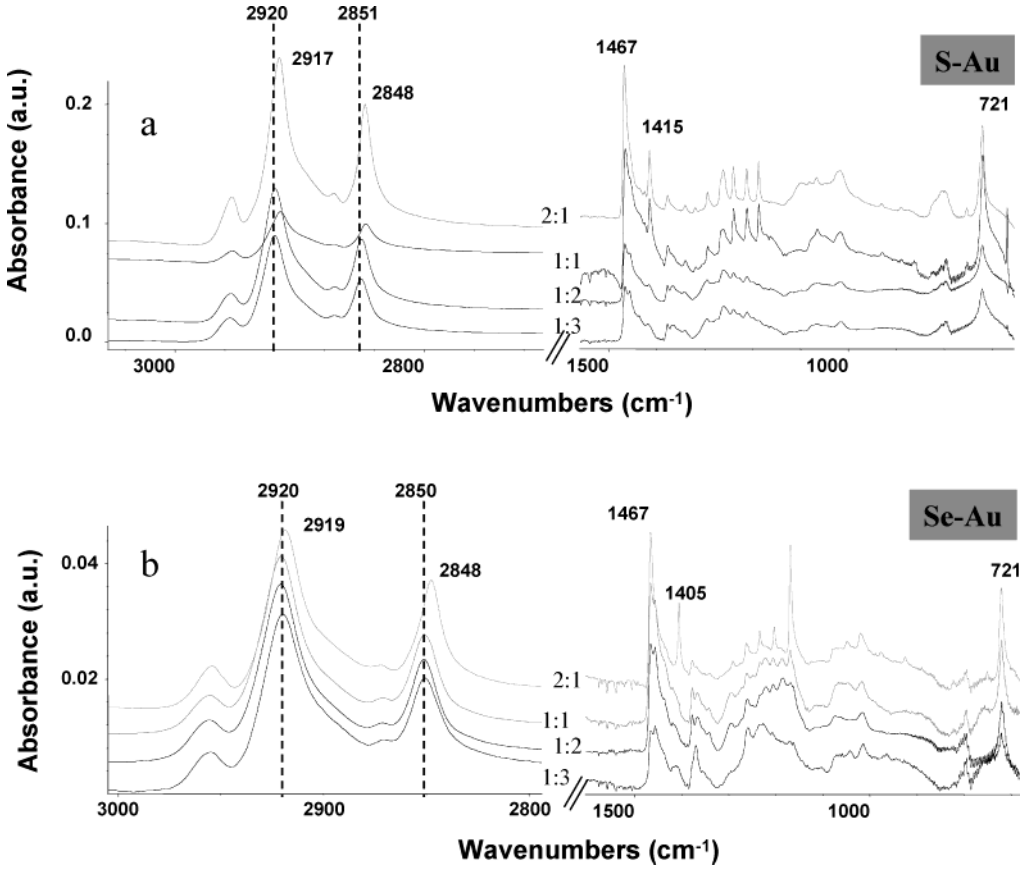

Figure 6. Shift of $\upsilon_s(CH_2)$, $\upsilon_{as}(CH_2)$, and the twisting−rocking, wagging progression bands for Au/DDT (a) and Au/DDSe (b) nanoparticles in four different mole ratios. The FTIR spectrum was taken at room temperature.

Au and DDSe/Au series. As mole ratios decreased, that is, 1:2 and 1:3, the progression bands became broader and less well-defined. This observation establishes that, for low mole ratio nanoparticles, the chains are more conformationally disordered and consistent with the trend inferred above that, for both DDT/Au and DDSe/Au, the assembly of chains becomes disordered as mole ratios are lowered in the starting reaction mixtures.

To examine the effect of preparation temperature on ligand or monolayer properties at the nanoparticle surfaces, we prepared DDSe/Au and DDT/Au nanoparticles at two well-separated temperatures, namely 6 and 25 °C, at the 1:1 mole ratio. FTIR spectra for these two series of samples are shown in Figure 7. These data show that as the preparation temperature was changed from 6 to 25 °C, the υ_{as} and υ_{a} stretching bands of DDSe/Au shift from 2920 to 2917 cm^{-1} and from 2851 to 2848 cm^{-1}. For DDT/Au, the υ_{as} and υ_{a} stretching bands were 2915 and 2847 cm^{-1}, respectively, at 25 °C, in comparison with 2918 and 2848 cm^{-1} observed at low temperature. These data clearly show that at near ambient temperatures the DDT/Au and DDSe/Au nanoparticles possess conformationally ordered, crystalline-like chains at their surface.

X-ray photoelectron spectroscopy was used to determine the ligand−substrate bond characteristics, namely S−Au and Se−Au linkages, for the DDT/Au and DDSe/Au. These data are shown in Figure 8**.** A sharp doublet with a peak-to-peak distance of about 3.65 eV was observed in all Au/DDT cases for the Au 4f level; the representative case (2:1) was shown in Figure 8d. Binding energies of 84.2 and 84.4 eV (Figure 8a) for Au/DDT and Au/DDSe, respectively, were recorded for the $4f_{7/2}$ peak, indicating the absence of Au(I). (The presence of Au(I) necessarily requires a shoulder on the Au^0 $4f_{5/2}$ peak near 84.9 eV,

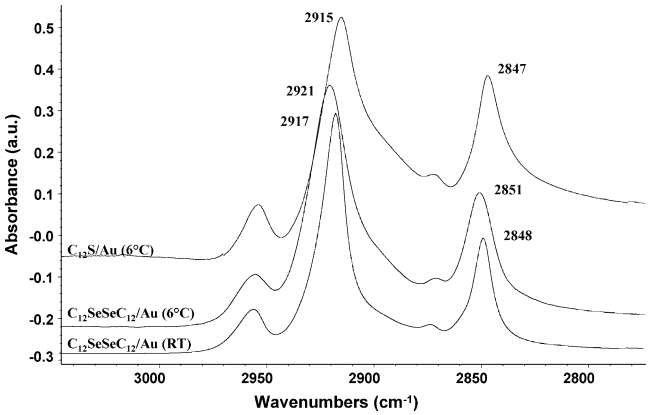

Figure 7. C−H stretching vibrations in the FTIR spectra of DDSe/Au and DDT/Au nanoparticles prepared at 6 and 25 °C referenced to the spectrum of DDT/Au (not taken) at 25 °C reported in the literature.

according to Heath and McNeillie.[21,22]) Although the estimation was conservatively made by the above two groups that, under some uncertainty, <8% of charged Au, if any, should exist in an ionized state on the surface, most of the ligand/Au interactions were expected to be neutral, or charge counterbalanced by both species.

The binding energy of the S $2p_{3/2}$ peak (Figure 8e) was 162.9 eV for Au/DDT. This value is relatively lower than those found for the free thiols (163.3−163.9 eV),[23,24] and it is consistent with values reported for thiolates binding

(21) McNeillie, A.; Brown, D. H.; Smith, W. E.; Gibson, M.; Watson, L. *J. Chem. Soc., Dalton Trans.* **1980**, 767.
(22) Leff, D. V.; Brandt, L.; Heath, J. R. *Langmuir* **1996**, *12*, 4723.
(23) Bain, C. D.; Blebuyck, H. A.; Wbitesides, G. M. *Langmuir* **1989**, *5*, 723.

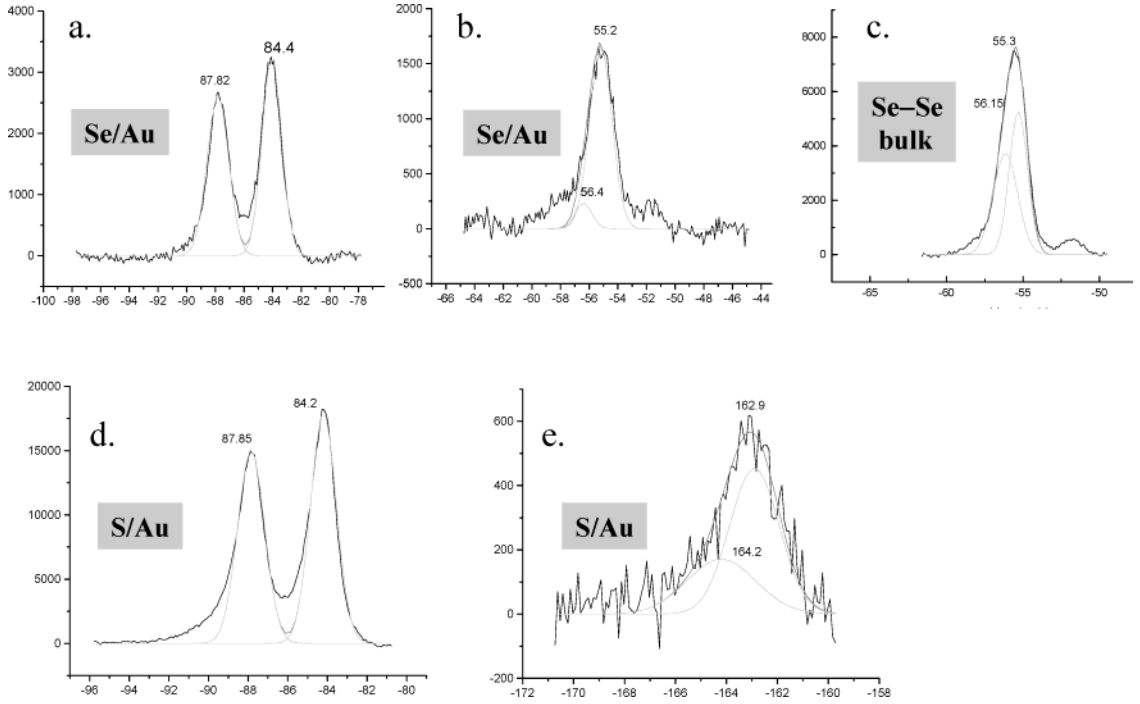

Figure 8. XPS investigation on Au/DDSe nanoparticles [(a) Au $4f_{7/2}$; (b) Se $3d_{5/2}$; (c) Se $3d_{5/2}$ in bulk $C_{12}Se-SeC_{12}$] and Au/DDT nanoparticles [(d) Au $4f_{7/2}$; (e) Se $3d_{5/2}$.

to gold (162.0−162.4 eV).[23,25] The lower binding energy trend (free thiols $^{(bulk)}$ > Au/DDT) of the S $2p_{3/2}$ peak suggested that there is much less covalent character to the Au−S bond in Au/DDT than to the S−S bond in the free thiols, indicating the covalent S−S bonds were cleaved upon binding to gold nanoparticles. As for Au/DDSe, the binding energy of the Se $3d_{5/2}$ peak (Figure 2b) was determined to be 55.2 eV, as compared to that of the bulk DD_2Se_2 (55.3 eV, Figure 2c), that is, the same value within the experimental error, suggesting a stronger, more covalent Au−Se bond in the nanoparticles.

Discussion

The wide range of characterization presented here establishes that alkyl selenoate provides an attractive alternative to alkanethiols as a useful ligand in the synthesis of Au nanoparticles. Well-defined alkaneselenoate monolayers at gold via surface self-assembly were previously shown by Samant and co-workers.[10a] This work serves to demonstrate that the same self-assembly can be employed to controllably synthesize gold nanoparticles. The DDSe/Au nanoparticle synthesis was carried out in a one-phase process by reducing $H[AuCl_4]$ in THF, in the presence of didodecyl diselenide (DD_2Se_2) using lithium triethylborohydride (superhydride) as the reducing agent at 6 °C for a series of ligand/substrate precursor mole ratios. But two-phase synthesis using toluene/water and room temperature reaction also proved successful. The formation of DDSe/Au was confirmed by the TEM and UV absorption spectroscopy data, and the presence of the DDSe ligand was revealed directly by the FTIR spectroscopy and XPS data and indirectly by the TGA data—all presented above.

A key finding of the present study was that control of particle size for the thiolate-stabilized Au nanoparticles could be achieved simply by varying the mole ratio of ligand to substrate precursors in the starting reaction mixture. Selenoate-stabilized Au nanoparticles, however, did not display such simple tunability. DDT/Au nanoparticle sizes could be varied from 2.6 to 5.1 nm by altering the mole ratios from 2:1 to 1:3. By contrast, DDSe/Au nanoparticles remained uniform at ∼2.5 nm for all reactant mole ratios in the one-phase synthesis. However, when the toluene/water-based, two-phase synthesis approach was used in a control experiment, we noticed large and dramatic variations in particle size (and even shapes and distribution) when reactant mole ratios were changed.

The observed mole ratio dependence of the particle sizes for the thiolate-stabilized nanoparticles can be straightforwardly understood in terms of the self-assembly of thiolate chains terminating the cluster growth. At higher mole ratios, the greater availability of ligands would limit the growth of the nanoclusters to smaller sizes, and conversely, at lower mole ratios, the lower concentration of ligand slows the self-assembly process, thereby allowing the Au clusters to grow to larger dimensions. This notion is supported by the ligand occupancy or density information in the data presented. At high ligand to substrate mole ratios, higher density for alkanethiol chains on nanoparticles was evident from the weight loss measurements in TGA and further supported by the higher integrated intensities observed for the chain vibrational modes in the FTIR spectra.

This apparently simple explanation, however, fails to account for the observed uniformity in selenoate-capped Au nanoparticles where the TGA and FTIR data reveal higher ligand densities for higher reactant mole ratios. We speculate this apparent contradiction to result from large discrepancies in the ligand self-assembly and gold-clustering reaction rates for the DDSe/Au case.

One possible hypothesis could be that due to slower self-assembly rates a larger amount of nanoparticles of similar sizes had actually nucleated as gold content increased from 2:1 to 1:3 instead of gradually growing in size. Thus, a similar surface area has now become available for less number of alkaneselenoate moieties to be attached

(24) Nuzzo, R. G.; Zegarski, B. R.; Dubois, L. H. *J. Am. Chem. Soc.* **1997**, *109*, 7733.
(25) Fabianowski, W.; Coyle, L. C.; Weber, B, A.; Granata, R. D.; Castner, D. G.; Sadownik, A.; Regen, S. L. *Langmuir* **1989**, *5*, 35.

Table 1. Elemental Analysis of Au/DDSe Nanoparticles Obtained by Inductively Coupled Plasma Optical Emission Spectroscopy (ICP-OES)

sample	% C	% H	% Au	% Se
Se/Au (2:1)	29.19	5.11	49.23	16.36
Se/Au (1:1)	23.35	3.82	60.16	13.12
Se/Au (1:2)	3.78	0.65	93.39	2.00
Se/Au (1:3)	1.92	<0.5	95.78	0.98

in the case of 1:2 and 1:3; hence, chains become less well packed. Consequently, existence of voids and defect sites becomes more common and likely. As a result, both ordered and disordered chain packing domains could coexist (Figure 3c and d), each revealed by a different type of desorption mechanism, such as seen in the TGA data. Indeed, conformational information derived using FTIR peak positions for the ligand chains supports the notion that less dense and a more disordered average ligand chains cover the nanoparticle surface when the mole ratios are lowered.

As these two step transitions were further examined in terms of percent of weight loss, onset desorption temperature, and inflection point for each transition process, the above scenario became quite logical and plausible. With less number of chains available, the tendency of forming well-ordered domains would have declined (3.26%/2.89% in 1:2 and 1.69%/1.54% in 1:3). Collectively, the existence of more well packed domains in 1:2 resulted in a relatively higher onset desorption temperature (129 °C) and a higher point of inflection than that in the 1:3 case. For confirmation, the trace of Se and Au in each mole ratio was obtained by inductively coupled plasma optical emission spectroscopy (ICP-OES) (Table 1), which additively complied to the above scenario by revealing an abrupt decrease in Se/Au ratio between 2:1 and 1:3 and a gradual decrease between 1:2 and 1:3 while C/Se ratios were approximately the same over all cases.

Specific details of chain conformation, packing, interdigitation, and the overall chain stability for both DDSe/Au and DDT/Au nanoparticles were established using FTIR and TGA data. The FTIR evidence proved that the chain ordering decreased as mole ratios decreased from 2:1 to 1:1 to 1:2 to 1:3 for both series. At the highest mole ratios, nearly all-trans chains, with little or no conformational defects, were evident, and at lower mole ratios both DDSe/Au and DDT/Au exhibited accumulation of a small but nonvanishing population of gauche defect conformer. We also note that, for each reactant mole ratio, the thiolate chains exhibit a slightly higher degree of order than the corresponding selenoate analogues at the corresponding mole ratios. Since TGA data reflect the overall chain stability resulting from both chain packing and headgroup−substrate interaction, the higher thermal stability (higher onset desorption temperature) of the alkaneselenoate chains in 2:1 ratio where chain densities are comparable would logically imply a stronger ligand−substrate interaction at the surface. This became clearer in the XPS data discussed below.

The thermal behaviors of alkyl chains on Au/DDSe and Au/DDT nanoparticles at two temperatures have been examined using FTIR spectroscopy (Figure 6). The mole ratio used was 1:1. As observed from the FTIR spectra, chains are oriented and packed in a much more ordered fashion when the Au/DDSe nanoparticles are synthesized at 25 °C. For Au/DDT, the molecular chains at 6 °C depicted higher order and crystallinity compared to those reported by Murray and co-workers (υ_{as}, 2918 cm^{-1}; υ_{a}, 2850 cm^{-1}) for Au/DDT synthesized at 25 °C. These data suggest that the dependence of the chain ordering is just opposite to that observed for Au/DDSe.

All above observations may have suggested that the anchoring rigid headgroup, RS- or RSe-, may have influenced the chain behaviors on nanoparticle surfaces. The XPS results provide some insight into the packing and ordering processes for nanoparticles prepared at the two temperatures. XPS suggests that the Au−Se bond is less ionic than the Au−S bond. The fact that alkyl chains on Au/DDSe are more organized in nanoparticles prepared at 25 °C may suggest that the ordering process requires activation energy. If ordering involves mobility of adsorbed DDSe moieties, this should be more facile at 25 °C than at 6 °C. In the case of DDT moieties, it was found that mobility requires increased charge separation, since the charge at the thiolate sulfur when it is at the on-top site of a Au(111) surface is 0.7 e, while at the hollow site it is 0.4 e.[26] Hence, moving from one hollow site to its neighbor requires an increase in charge separation. The XPS results suggest that this was not the case for the Au−Se bond, since there is no apparent charge separation to begin with. This implies that the mobility of DDSe moieties will require lower activation energy than that of the DDT counterparts.

The case of Au/DDT is different due to a radically different mechanism involved in its formation. There, Au−DDT bonds are established *in the precursor polymer*, and the formation of nanoparticles upon reduction requires the breaking of Au−S bonds, so that gold atoms can become part of the particle core. The lower temperature is associated with less disordered chains (gauche defects) and thus better packing and ordering during formation.

The above discussion can be reconciled in terms of a unifying mechanism for the selenoate-stabilized nanoparticle formation. It appears reasonable to propose that while thiols reduce Au^{3+} to Au^{1+} and form a thiolate/gold polymer intermediate, the Se−Se bond does not undergo cleavage when DD_2Se_2 is mixed with the Au^{3+} precursor. Rather, THF stabilized the formed gold nanoparticles, and DD_2Se_2 reacts with these nanoparticles via an oxidative addition mechanism, similar to the reaction of RS−SR with gold substrate during the formation of a self-assembled monolayer. Bandyopadhyay and co-workers have suggested, on the basis of Raman spectroscopy studies, that while the S−S bond in diphenyl disulfide dissociated upon adsorption of gold surfaces, the Se−Se bond in diphenyl diselenide remained intact.[10c]

This hypothesis can be easily confirmed simply by examining the color of the reaction mixture prior to reduction. Indeed, while the color turns darker every time a thiol is added to the Au^{3+} precursor, no color change was observed when DD_2Se_2 was added, suggesting that no coordination complex intermediate had been formed. The THF has a dual role in this reaction. First it coordinates with the Au^{3+} ions, thus replacing the chlorides, resulting in the complete solubility of $H[AuCl_4]\cdot 4H_2O$. Second, it acts as a surfactant, stabilizing the formed gold nanoparticles and thus preventing excessive agglomeration. This dual role suggests that the THF molecules that solvated Au^{3+} ions continue to be coordinated to the Au(0) at the nanoparticle surface, very much like thiolate groups. Therefore, the resulted size distribution becomes rather uniform. Toluene, on the other hand, is a nonpolar organic solvent that displays none of the above characteristics; it could not play the role of solvation of nanoparticles before/

(26) Sellers, H.; Ulman, A.; Shindman, Y.; Ellers, J. E. *J. Am. Chem. Soc.* **1993**, *115*, 9389. (b) Beardmore, K. M.; Kress, J. D.; Gronbech Jensen, N.; Bishop, A. R. *Chem. Phys. Lett.* **1998**, *286*, 40.

during reduction. Under ligand abundant condition (Figure 1i, 1:1), the molecular chain served as the solvation agent, thus preventing the particles from aggregating. However, when the selenoate concentration attenuated much further in the 1:3 case (Figure 1j), without any solvation, Au(0) agglomerated massively, thus resulting in random particle sizes and a broad size distribution.

Conclusions

Alkanethiolate chains packed more orderly on gold nanoparticles than their selenoate analogues, as illustrated by FTIR spectroscopy. The binding energy of the Au−Se bond was found to be slightly higher than that of the Au−S bond, on the basis of the XPS studies. Alkaneselenoate chains interact more strongly with gold than their thiolate counterparts in higher mole ratios, as illustrated by the resulted higher desorption temperatures. The particle size of DDT/Au showed a strong dependence on the reactant mole ratios, whereas that of DDSe/Au exhibited no significant dependence. A different mechanism was proposed, where DD_2Se_2 molecules do not form a "polymer-like" intermediate with gold ions before reduction, as DDT does. This phenomenon, together with the observed solvent and temperature effects, explained the influential effects of particle size and size distribution on the ultimate chain conformation and packing order at particle surfaces.

Acknowledgment. This work was funded by the NSF through the MRSEC for Polymers at Engineered Interfaces. The work at Los Alamos National Laboratory was supported partially by the LDRD program.

LA020628I